

# Understanding climatic traditions: A quantitative and qualitative analysis of historic dwellings of Cadiz

Carlos Rubio-Bellido<sup>1</sup>, Jesús A. Pulido-Arcas<sup>2</sup>  
and Jose M. Cabeza-Lainez<sup>3</sup>

## Abstract

Many historical European cities are home to houses of great heritage value. These structures have been able to provide comfort throughout history without the use of artificial conditioning systems. Even though such dwellings were influenced by academic styles, by contradicting vernacular architecture, their adaptation to local climate in order to achieve thermal comfort is commonplace. They were mostly built within compact urban tissues, making use of local materials, workforce and construction technologies. Learning from the past knowledge of these design strategies that are specifically adapted to specific climates can play a significant role in reducing the energy demand of extant buildings. Likewise, this paper thoroughly investigates the remaining urban conglomerate of Cadiz from a scientific approach. An original simulation software, duly tested with on-site measurements, was used to analyse the passive design strategies that were applied effectively. The results of this study indicate that historic neighbourhoods in Cadiz are creatively adapted to their natural conditions. In this sense, the main conclusion is that in mild climates, the combination of a compact urban tissue and climate responsive dwelling design should be sufficient to maintain acceptable indoor comfort levels.

## Keywords

Climate responsive design, Historic architecture, Simulation and software, Traditional building techniques, Bioclimatic design

Accepted: 13 November 2016

## Introduction

In recent years, the depletion of energy resources and the risk of global warming have imposed a new path for human development based on both the use of renewable energies and the improvement of energy efficiency. It is commonly acknowledged that the building sector accounts for one-third of the total gross energy consumption worldwide. In Europe this sector, which includes households and commercial buildings, accounts for 37.4% of the final energy consumption and shows an increasing tendency for the near future.<sup>1</sup> A recent report from the Spanish National Energy Plan foresees that, if energy consumption were to be reduced to counteract the effects of climate change, 15.6% of this decrease would correspond to the construction sector.<sup>2</sup> For this reason, it is essential to appraise the main characteristics of a large part of the existing building stock, which

corresponds to structures that rather than relying on artificial air-conditioning are designed on the basis of climate adaptation.

Nowadays, historic cities provide useful lessons for achieving sustainable development, even without

---

<sup>1</sup>Department of Building Construction II, Higher Technical School of Building Engineering, Universidad de Sevilla, Seville, Spain

<sup>2</sup>Department of Building Science, Faculty of Architecture, Construction and Design, Universidad del Bío-Bío, Concepción, Chile

<sup>3</sup>Higher Technical School of Architecture, Universidad de Sevilla, Seville, Spain

### Corresponding author:

Carlos Rubio-Bellido, Department of Building Construction II, Higher Technical School of Building Engineering, Universidad de Sevilla, Avenida Reina Mercedes 4A, Seville 41012, Spain.  
Email: carlosrubio@us.es

compromising modern living standards. Regarding this matter, from the very first research that arose in the 1960s, the scarcity of natural resources enhanced the climate adaptation of what was called ‘modern vernacular architecture’ using local materials.<sup>3,4</sup> Several studies have proven that vernacular architecture is able to reduce energy consumption and achieve thermal performance.<sup>5–7</sup> However, an understanding of historic dwellings based on a mixture of traditional and academic influences located in dense urban areas becomes a necessity in this field of study.

The majority of research in the area of climate responsive design focuses on qualitative analysis and takes into account the relationship between building shape, materials, construction techniques and local climate. Despite this fact, various authors strive to use numerical models considering energy performance evaluation of vernacular architecture all over the world,<sup>8</sup> sustainable building strategies at regional scale<sup>9</sup> and using building information modelling technologies.<sup>10</sup>

A lack of proper computer-based simulations and on-site monitoring leads to several difficulties in understanding the actual performance of extant historic properties, as well as their capability of achieving comfortable indoor conditions. The need for documenting

such knowledge has been often coined as ‘learning from the past’;<sup>11–13</sup> from a scientific approach, both qualitative and quantitative assessments are essential to advance in this field of study.

The residential architecture of the historic city of Cadiz (36°32’N, 6°18’W) (Figure 1) has gradually evolved based on the principle of climate responsive design.<sup>14</sup> The influence of the balmy Mediterranean climate<sup>15</sup> due to its coastal location becomes evident in the pattern of early settlements. According to recorded data (Table 1), the climate in Cadiz is characterized by mild temperatures (average 17.5°C) (Figure 2) with a relevant amount of sunshine hours (2802 h/year), high relative humidity (RH) (73%) and a constant breeze ( $v < 4$  m/s), with only a few calm days. Summers are fairly warm and winters are not harsh, with scarce precipitation all year round. This favourable scenario predicts the feasibility of achieving comfort conditions with the sole use of climate responsive design.

The majority of the surviving traditional architecture of Cadiz dates from the 17th, 18th and 19th centuries, as the existing conglomerate was constantly transformed due to dynamic port activity. This urban tissue merged both vernacular and alien influences, which were the product of the rich trade both in

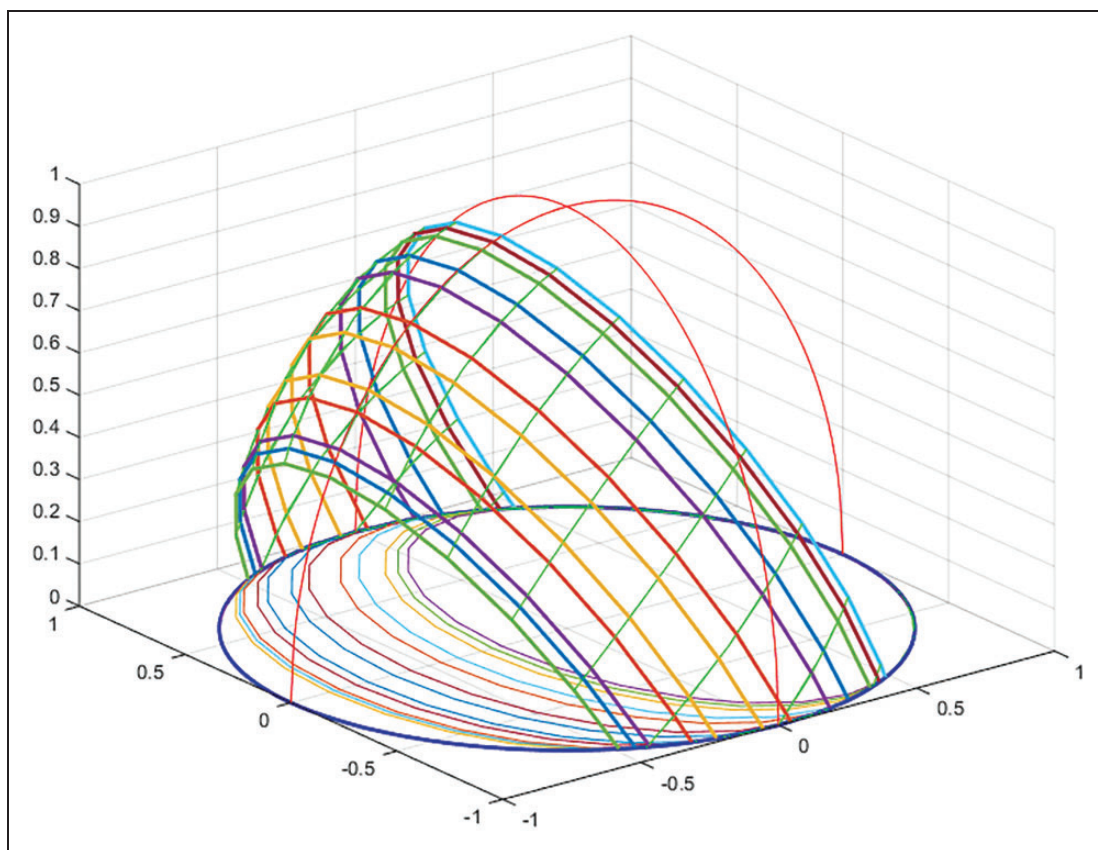


**Figure 1.** Annual 3D solar chart of Cadiz. DianaX®.

**Table 1.** Monthly normal climate of Cadiz.<sup>16</sup>

Months		Jan	Feb	Mar	Apr	May	Jun	Jul	Aug	Sep	Oct	Nov	Dec
Temperature (°C)	Max	15.6	16.4	18.2	19.3	21.7	24.9	28.1	28.5	26.4	22.6	19.0	16.6
	Min	8.4	9.1	10.1	11.3	13.6	16.4	18.8	19.3	18.0	15.1	11.8	9.9
	Mean	12.1	12.7	14.2	15.3	17.7	20.6	23.5	23.9	22.2	18.9	15.4	13.2
Rainfall (mm)		86.0	66.5	51.0	57.5	34.0	11.0	2.0	5.0	18.0	67.0	81.5	113.5
No. of rainy days		8	8	6	7	4	2	0	0	2	6	7	10
Relative humidity (%)		77.5	76.5	72.5	71.5	70.5	69.5	67.5	69.0	71.5	75.0	76.5	78.0
Sunshine hours (h)		167	171	216	231	281	297	330	317	246	215	179	152

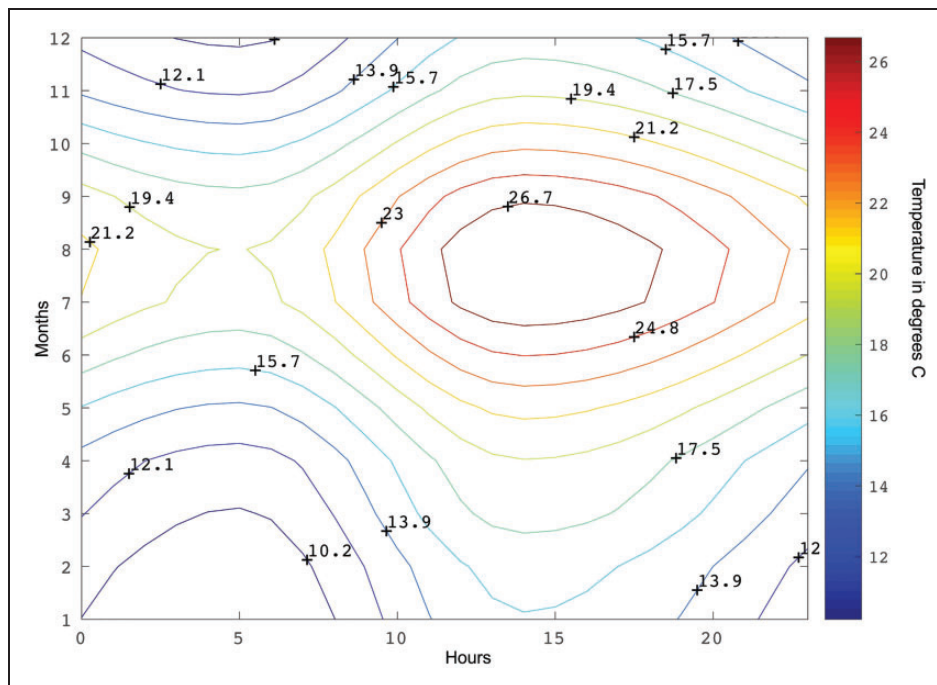


**Figure 2.** Annual isopleths of Cadiz. DianaX®.

commodities and ideas. The surviving urban conglomerate can be characterized as a compact district, traversed by labyrinthine streets and courtyards. What is more, urban life in the old quarter of Cadiz was notoriously influenced by climate, and the town maintains a tradition of intuitive building techniques, creatively adapted to the climate. This condition is similar to other Mediterranean cities, such as Ortigia in Siracusa (Italy) or the Spanish Quarter in Naples (Quartieri Spagnoli). With a general description of such an urban fabric, the following specific elements can be outlined: predominance of vertical openings in the façades, use of a central courtyard to organize and give access to dwellings, a high thermal mass envelope and varied elements for solar control like shutters, hangovers or louvers.

Despite this historic city having been the object of numerous studies, the absence of research that focuses on its climate adaptation is evident. Such architecture requires a comprehensive analysis in order to allow for a better understanding of its climate responsive design in terms of energy efficiency and sustainable design.

### Objectives and methodology

This research aims to clarify how climate responsive design is present both at the urban scale and in historic dwellings of Cadiz, in terms of indoor comfort conditions. The methodology used a specific simulation software, called DianaX®, self-developed by ourselves, and on-site fieldwork to obtain first-hand data. Through the statistical treatment of the formerly gathered data, the

main morphological and constructive features of these properties were defined. By comparing our simulation results with the on-site data, the necessary feedback was obtained to determine the environmental performance of these residential buildings.

The climate adaption in an urban context is rather difficult to predict, especially for street canyons in sunny climates if mainstream commercial simulation tools are used. This is due to the fact that a large amount of interreflection is generated inside this space as a product of the combination of clear sky conditions and highly reflective materials. For this reason, we conducted theoretical research on radiative transfer based on the theory of configuration factors for complex surfaces.<sup>17–19</sup> Outcomes were used to devise a simulation tool specifically adapted to the peculiarities of urban canyons,<sup>20</sup> which considers all possible sky conditions, as well as the amount of direct, diffuse and reflected radiation that is present inside the canyon itself. This tool was validated with field measurements in order to check its accuracy and also to quantitatively analyse the influence of a dense urban tissue on environmental performance of buildings.

Fieldwork was conducted from January to November 2009 to assess 88 heritage residential properties. As a result of this work, an ample database was compiled that was comprised of information about the urban grid, the morphology of houses, constructive systems and historical records, as well as graphical information (plans, historical drawings and photographs). The raw data were organized and categorized using data mining techniques in order to find the most predominant house typology. In this sense, according to previous research focused on the old quarter of Cadiz,<sup>21</sup> the main morphological features of these heritage properties have been identified as follows: a row house located on a plot with a front width of three spans and a depth of three spans, with a span averaging 5–6 m. The resulting plot has an approximate dimension of 18 m × 18 m and an area of approximately 300 m<sup>2</sup>. Building coverage ratio is very high, around 90%, as is floor-to-area ratio (FAR), at 400%. Starting from the main façade, the distinctive spatial system of these houses is composed of a central access in the first span, an approximately squared central patio, with dimensions of 5 m × 5 m located in the second span, and finally the main stairs located in the third span. This predominant property has four levels, topped with a flat roof.

Of the properties with the said characteristics, one was chosen as the objective of both computer simulations and on-site measurements. The house, located at 17 Jose del Toro Street, is very representative of the urban fabric of the old quarter of Cadiz in terms of building morphology. By virtue of the aforementioned

database, we could target those elements that are responsible for the climate responsive design strategies. In this case, the following have been identified as relevant in order to assess the historic housing of Cadiz in a qualitative manner: solar access, building morphology and characteristics of the thermal enclosure (walls, roof, ceilings and openings). In order to assess their effect on interior conditions, the simulations were carried out with the radiative exchange tool DianaX<sup>®</sup>,<sup>22</sup> which takes into account specific outdoor conditions and also considers radiant thermal asymmetries. In addition, long-term monitoring was undertaken in order to quantitatively verify the internal and the external contour conditions. This process includes measurements of dry bulb temperature and RH in a representative dwelling. Sensors were placed on the second floor, both indoors and outdoors, for a period of 10 days in a summer (from 7 to 17 July 2011) and a winter (from 10 to 20 January 2011).

Based on the ‘adaptive approach’, the comfortable temperature limits for naturally ventilated buildings are the outcome of our field studies which were based on ASHRAE standard 55-2013.<sup>13</sup> Thus, the plot of temperature (indoors and outdoors) (Figure 20) through the adaptive comfort model supports the hypothesis that these dwellings are effectively adapted to the local climate, and consequently are able to provide comfort with traditional design methods.

## Adaption to urban context

### Simulation tool for urban canyons

Radiant distribution inside the studied urban canyons was assessed using a self-developed simulation tool, whose calculation script was implemented in Matlab<sup>®</sup>.<sup>20,23</sup> This tool is essentially based upon former works by Lambert, Moon and Yamauchi amongst others.<sup>29–31</sup>

By making use of theoretical formulae on the field of radiant transfer between surfaces, a starting point was established on the basic canonical expression for radiative transfer, which responds to the integral equation (1)

$$\Phi_{1-2} = E_{b1} \left[ \int_{A_2} \int_{A_1} \frac{\cos \theta_1 * \cos \theta_2}{\pi * r^2} dA_1 * dA_2 \right] \quad (1)$$

Equation (1) is dependent on the angle  $\theta$ , distance  $r$  and area  $A$ , of the surfaces involved. The expression used in the calculation script was obtained by integrating this equation for several types of emitters. Equations (2) and (3) were used to calculate the radiant interchange between perpendicular and parallel surfaces, respectively:  $a$  and  $b$  represent the horizontal and vertical dimensions of the rectangular emitting

surfaces and  $y$  stands for the distance between the calculation point and the emitting surface

$$f(x, y) = \frac{E}{2} \left[ \frac{\arctan b}{y} - \frac{y}{\sqrt{a^2 + y^2}} \cdot \frac{\arctan b}{\sqrt{a^2 + y^2}} \right] \quad (2)$$

$$f(x, y) = \frac{E}{2} \left[ \frac{a}{\sqrt{a^2 + y^2}} \cdot \frac{\arctan b}{\sqrt{a^2 + y^2}} + \frac{b}{\sqrt{b^2 + y^2}} \cdot \frac{\arctan a}{\sqrt{b^2 + y^2}} \right] \quad (3)$$

Further information on the theoretical basis of these equations and the governing algebra used for calculations can be found in the work of Cabeza-Lainez.<sup>22</sup> Considering the specific simulation procedure for urban canyons, a thorough description of the numerical model and the Matlab<sup>®</sup> script can be found in Rubio-Bellido et al.<sup>20</sup>

With these expressions, the primary distribution of the radiant energy can be assessed. However, in order to establish an adequate approach for the reflections, equation (4) must be employed. For any receiving surface, the total component of the received radiation is the sum of the direct component and the reflected

component from the adjoining surfaces

$$E_{tot} = E_{dir} + \sum_n \cdot E_{ref} \quad (4)$$

Applying this expression to the geometry of the urban canyon, a parallelepiped space of six surfaces had to be constructed. In the expression depicted in equation (5),  $F_{ij}$  is the form factor between any surface  $i$  and  $j$  (plane or curved),  $\rho_i$  is the reflection coefficient of a given surface,  $E_{di}$  is the direct component of the  $i$  surface and  $E_{ri}$  is the reflected component of that surface

$$\begin{bmatrix} 1 & \cdots & -F_{16\rho6} \\ \vdots & \ddots & \vdots \\ -F_{61\rho1} & \cdots & 1 \end{bmatrix} \cdot \begin{bmatrix} E_{r1} \\ \cdots \\ E_{r6} \end{bmatrix} = \begin{bmatrix} F_{11\rho1} & \cdots & F_{16\rho6} \\ \vdots & \ddots & \vdots \\ F_{61\rho1} & \cdots & F_{66\rho6} \end{bmatrix} \cdot \begin{bmatrix} E_{d1} \\ \cdots \\ E_{d6} \end{bmatrix} \quad (5)$$

The compiled script allows for both numerical and graphical outputs, in the form of numerical arrays and surface plots, respectively (Figure 3), which can be

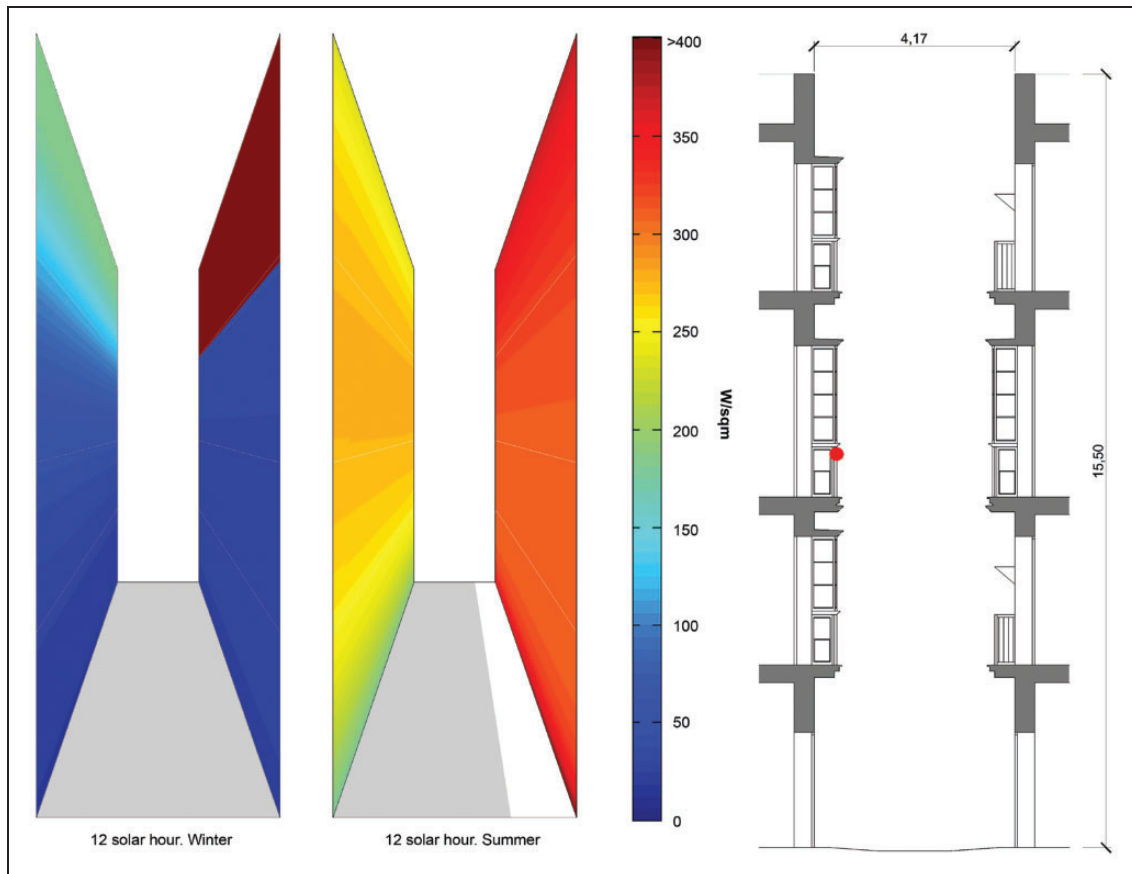


**Figure 3.** Simulation of façades N-E 28°, S-W 208°. Twelve solar hours in winter and summer.

easily incorporated into any given design. In this case, the radiant values of semi-open spaces such as urban canyons (partly composed of virtual surfaces ‘dubbed’ with a high absorption index) are considered crucial to the understanding of the radiant distribution inside the canyon.

The simulations were produced taking into account direct solar radiation as the primary energy source and the diffuse component reflected by surfaces as the secondary. Results are expressed in watts per square metre ( $\text{W/m}^2$ ), which can be assigned to thermal loads and internal gains of buildings.

### *Effective comparison between simulation data and field measurements*

Computer simulations were cross-checked against on-site measurements in order to validate both the calculation model and measurements themselves. One urban canyon representative in terms of its most important characteristics was chosen for the placement of measuring cells. It has a width of 4.17 m (5 varas) and a height of 15.5 m (Figure 4) and is oriented with a  $28^\circ$  deviation from the East–West axis. Accordingly, the majority of building façades are oriented either at  $28^\circ$  N-E or  $208^\circ$  S-W.

One measuring cell was placed on the  $28^\circ$  North-East façade, 8.2 m above the ground plane for the collection of data in winter and summer. Figure 5 depicts the comparison between theoretical values of radiation calculated using the aforementioned script and actual measurements. Additionally, for the sake of clarity in the discourse, data for the open field have also been included, as it was considered convenient to show the comparison with open field conditions in order to appraise the real effect of the urban grid on the availability of solar radiation.

A comparison of simulated and measured data clearly shows the positive effects of urban geometry on conditions of solar access during the winter period, when referring to buildings whose façade faces  $28^\circ$  N-E (Figure 7). The open field shows a maximum value of around 7:00 solar hours, as this is the time when, according to its orientation, this façade should receive the maximum diffuse radiation; from this moment, levels start to steadily decay to zero. The reason for this is the absence of direct solar radiation at this time of year. The reflected component from the opposite façade was shown to account for a considerable amount of the diffuse radiation, particularly between 8:00 and 15:00, when values can be twice as large as those in the open field.

In summer, the effect of urban geometry on the distribution of solar radiation is clear in the form of an overall decrease in levels. During early morning,



**Figure 4.** Section of typical street canyon and measuring cell.

sunrays impinge upon the  $28^\circ$  N-E façade directly, reaching a maximum of  $537.09 \text{ W/m}^2$  at 7:30, and from this point plummet to a value of  $60 \text{ W/m}^2$ ; then, as a result of the diffuse component coming from the sky vault, the curve in Figure 7 takes a smooth shape, decreasing slowly until sunset. In this season, rays of sunlight are blocked by the opposite façade during the morning. Therefore, the solar radiation values are due to the diffuse component and fall under  $100 \text{ W/m}^2$ . However, this tendency is inverted when the opposite façade is hit entirely by direct radiation and begins to work as a solar reflector. At this time, values from the N-E façade reach  $260 \text{ W/m}^2$ , about four times those expected in the open field.

The correlation coefficient between simulated and measured values was calculated (Figure 6). These value ranges between 0.9407 in summer and 0.9321 in winter, thus representing the expected values with a confidence interval of 93–94%. The root mean square error are  $23.71 \text{ W/m}^2$  in summer and  $10.37 \text{ W/m}^2$  in

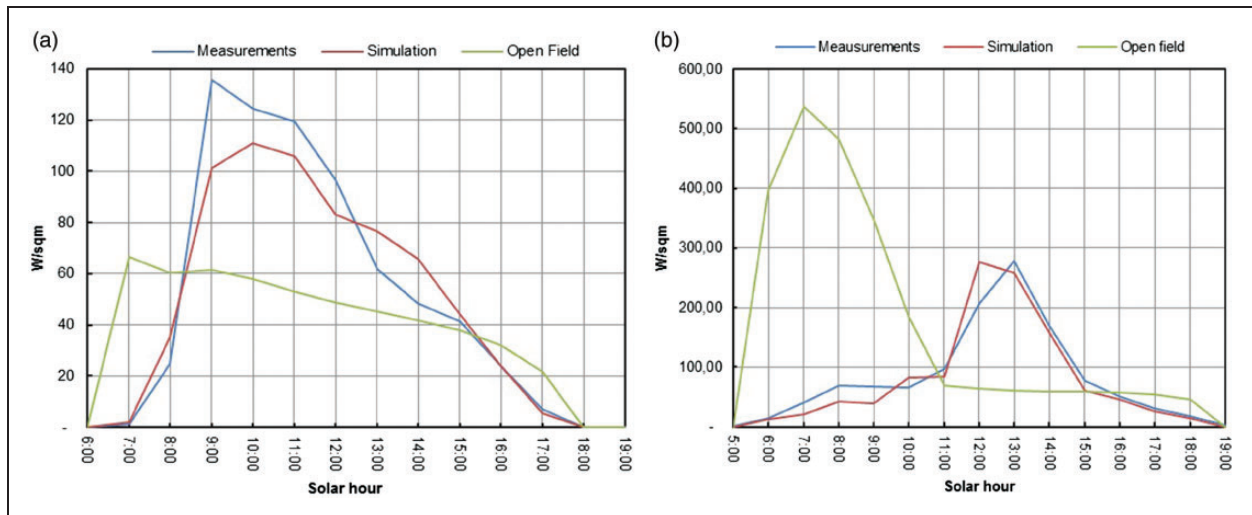


**Figure 5.** Comparison between cell measurements and simulations: (a) winter N-E 28° façade, 8.20 m height and (b) summer N-E 28° façade, 8.20 m height.

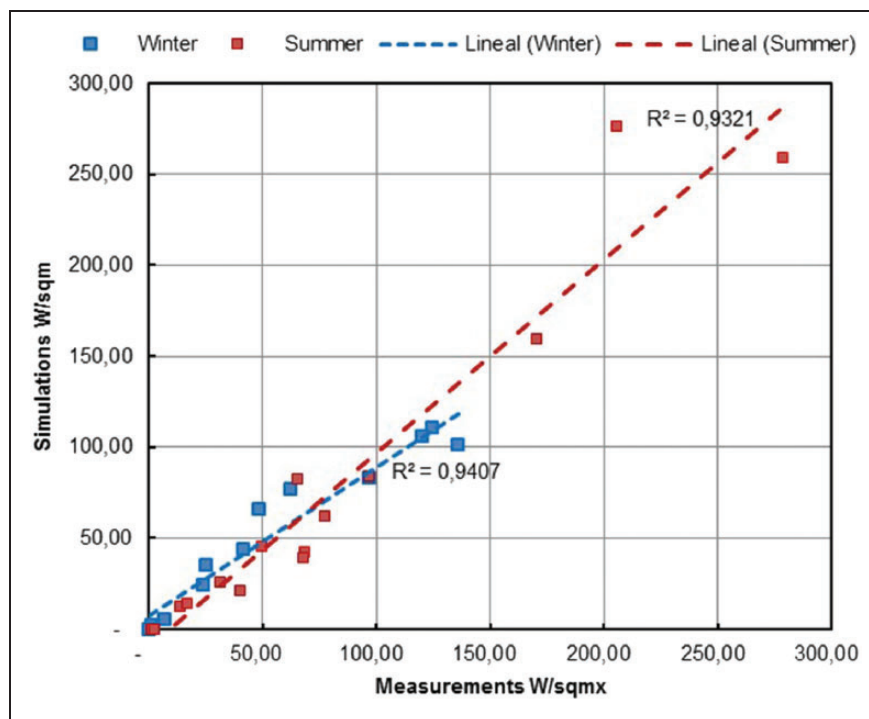


**Figure 6.** Regression simulation versus measurements: in winter and summer N-E 28° façade, 8.20 m height.

winter, and the normalized root mean error square deviation are 8.58% and 9.32%, respectively. On the contrary, some inaccuracies were found that can be explained by the following facts: first, geometrical singularities present in real buildings are not considered in the simulation model; second, some theoretical values

for these reflection coefficients (reflectance of the façades set at 0.6) are a weighted average value of all coefficients for different materials constituting the façade; and finally, the spectral response of the measurement cell may have a minor bias of approximately 5% in the presence of high temperatures.

### Simulations at various heights

Year round, low radiation levels have been found on the N-E façade (Figure 7), except for isolated peaks when penetrated by direct beams. Regarding winter conditions, poor radiation levels should be expected considering openings in this façade. However, this is only true for the open field and first floor of buildings located within the urban canyon, where values are always below  $62 \text{ W/m}^2$ . During this season, the opposite façade enjoys higher radiation levels by virtue of its reflective properties. On the second floor, values range around  $100 \text{ W/m}^2$  and on the third floor,  $200 \text{ W/m}^2$ . In summer, the overall effect of reduction on the level of solar radiation is also evident and was already

mentioned. Therefore, with a lower height, a lowering of figures were found. Urban geometry acts as a kind of solar protection that helps to reduce solar gains in the early morning. After midday, the opposite effect becomes evident, as levels in the canyon are higher than in the open field; the pattern of decay varies in accordance to the height of the simulated point.

On the other hand, the  $208^\circ$  S-W façade shows the typical behaviour for this orientation (Figure 8), which is beneficial in terms of environmental performance. Values during summer are around  $450 \text{ W/m}^2$ . This is evidently lower than those found in winter, which are around  $900 \text{ W/m}^2$ . In this case, the effect of urban geometry means an overall reduction in radiation

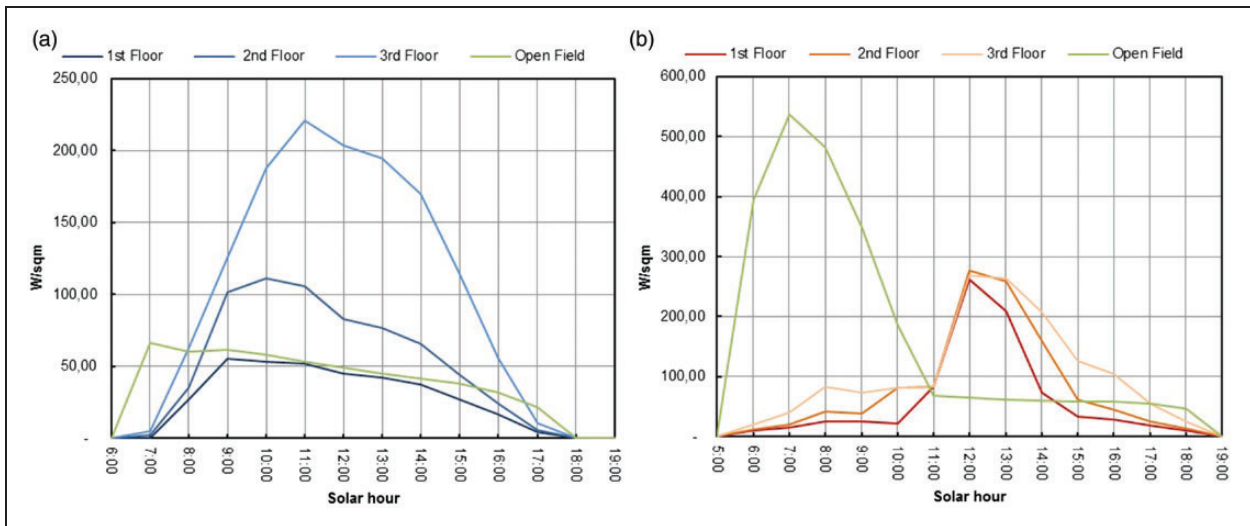


Figure 7. Simulation (a) winter  $28^\circ$  N-E façade various heights and (b) summer  $28^\circ$  N-E façade various heights.

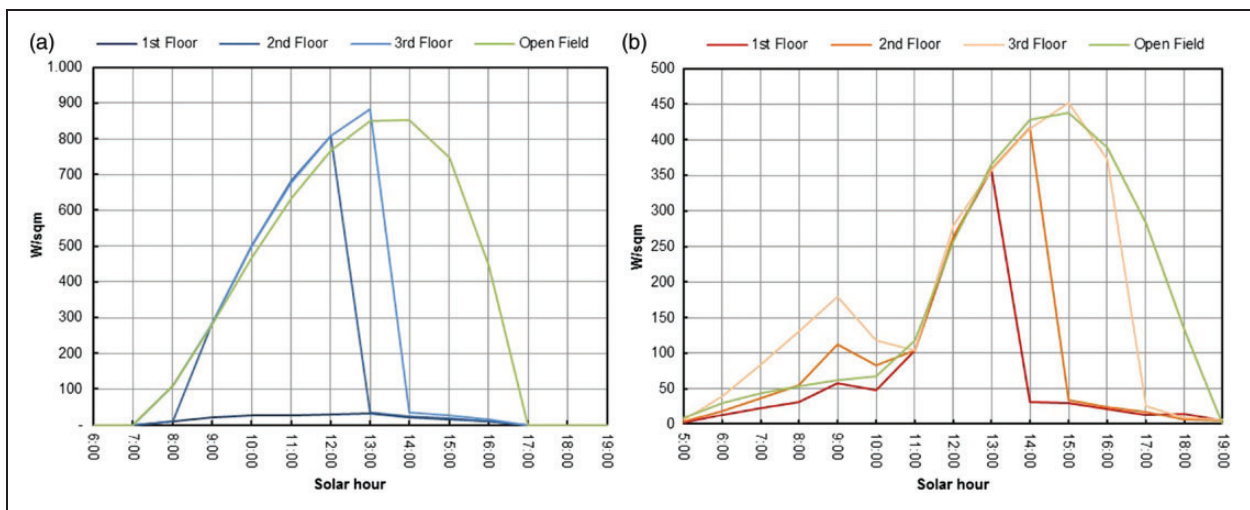


Figure 8. Simulation (a) winter  $208^\circ$  S-W façade various heights and (b) summer  $208^\circ$  S-W façade various heights.



levels for all seasons. In winter, the open field shows a typical sinusoidal distribution in accordance with solar trajectory, whereas points located within the urban canyon show a curve that falls abruptly due to the effect of the urban geometry. Each curve falls according to the height of the given point and afterwards levels are substantially low, with a maximum of  $32 \text{ W/m}^2$ . In summer, morning hours show a steady increase in radiation levels. Then a peak value is achieved in the afternoon. The point where the maximum value was found to deviate on the location of the point in question.

Urban geometry has a double effect on results shown in Figure 7. During morning hours, the reflected component of solar radiation from the opposite façade causes levels to increase from around  $62.50 \text{ W/m}^2$  (open field) to  $112.70 \text{ W/m}^2$  (second floor) and  $179.70 \text{ W/m}^2$  (third floor). In the afternoon, peak values were found at around 15:00 for the open field, while levels at other floors fell abruptly depending on the time when direct beams become obstructed by the opposite façade.

## Climate adaption of architecture

### *Building morphology and constructive systems*

Based on results of fieldwork, the prevalent type of historic dwelling was established (Figure 9): row houses, with plots of varying dimensions, dating from the 17th century.<sup>24</sup> Although the courtyard proportion appears relatively narrow, this is usually wider than adjacent streets. The building heights are habitually set at four

storeys, which has contributed to a uniform image of the street front. Except for a few singular plots located around public squares where representative public buildings are located, the majority of residential buildings have this configuration.

### *Envelope*

The load-bearing walls of the historic houses in Cadiz are mostly made of porous stone, a sedimentary rock composed of the remains of seashells found in the bay area. They are built with the traditional technique of ashlar and lime mortar and their thickness ranges between 50 and 60 cm in the ground and first floors. In certain buildings, stone masonry can be found in the second floor, whereas in other properties, especially buildings from the 18th and 19th centuries, masonry or solid bricks ( $30 \text{ cm} \times 15 \text{ cm} \times 5 \text{ cm}$ ) are used and decrease in thickness in accordance with building height. However, solid bricks are commonly found, only in the third floor, in order to reduce the section of the wall. Light-coloured tones are commonplace in the façades, which mix lime and clay and feature many hues. Regarding their thermal properties, these walls are characterized, more than by thermal conductivity, by their high thermal mass, high damping and thermal stability, thereby resulting in the attenuation of the energy effectively transferred to the inner side of the wall. These three combined characteristics could greatly help to keep the interior temperature nearly constant. Hence, thermal inertia also plays an important role in this kind of building.<sup>25</sup> Such high values produce a greater thermal stability, which in principle would be

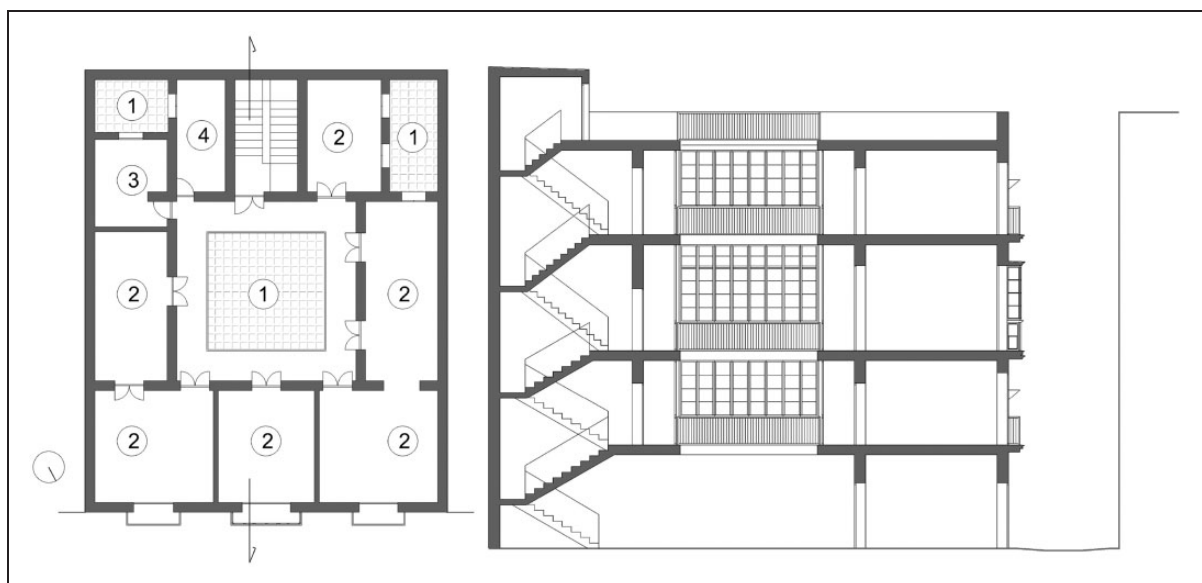


**Figure 9.** Plan and section of a typical dwelling in the city of Cadiz. 1 – courtyard, 2 – room, 3 – kitchen and 4 – bathroom.

a desirable feature, especially in climates whose temperature range is close to comfort conditions.

The flat roof common in Cadiz architecture is composed of various layers and supported by the structure of the last floor. From the interior to the exterior, its constructive system can be described as follows: waterproofing made of a clay and lime mixture, laid over bricks; a layer of volcanic ash that acts as a lightener for dead loads; an additional layer of clay and lime; and ceramic tiles set over a lime mortar layer. Most roofs have the same height, which results in a uniform building height, and hence the absence of solar obstructions. The only obstructions of note are the parapets belonging to these houses themselves and some individual elements, such as sea-facing turrets. Despite the fact that this is the building element that receives the greatest amount of solar radiation, its thermal performance is similar to that of the walls. This thermal inertia and stability could produce a tight range of indoor temperatures.

### Openings

The balcony (Figure 10) is one of the characteristic elements of these buildings, as well as one of the iconic images of the city. Except for the ground floor,

it is present on all levels of the façades. This opening is much more frequent than windows, which are found only in scarce locations and always on the last floor. They usually span from 1.00 to 1.20 m with a height of 2.20–2.40 m. This opening includes various layers from the outside to the inside and follows this sequence: exterior rolling louvers and adjustable shutters, hinged windows, textile curtains, interior hinged shutters and curtains. Thus, these openings are complex filter, with a large number of combinations in order to better adapt to changing outdoor conditions.

The glazed balcony (Figure 11), the other predominant type of opening, is widely present in the city, especially the Isabelline style. The complex frame that protrudes over the railing is inserted in the balcony itself. This design is unique and is not found in other nearby locations in Southern Spain. Its environmental performance differs from double glazed openings, since its mode of operation also involves heat accumulation in the intermediate space, which in turn, has a significant effect on the thermal inertia of the whole enclosure. Curtains are usually attached to the inner side of the glazing. In order to delimitate the interior space of the room, dense wooden doors are opened during the day. Generally, glazed balconies are very advantageous regarding energy performance, and work as attached



**Figure 10.** Balcony.



**Figure 11.** Glazed balcony.

greenhouses that create a buffer space, which in turn reduce conduction losses, thus generating comfort conditions when outside temperatures do not fall abruptly. They also store heat during winter thanks to the solar radiation gains obtained through glazed elements, as well as the thermal inertia of walls.

### Winter results

In winter, indoor air temperature stays nearly constant when compared to the oscillation of exterior temperatures (Figure 12). The outdoor temperature in the street canyon has a daily variation of 5°C, i.e. from 11.5°C to 16.5°C, and in the courtyard of about 4°C, while the indoor temperature varies from 17°C to 18°C, with a daily fluctuation of only 1°C (Figure 12).

As a consequence of thermal inertia, internal gains and solar gains, indoor temperatures could greatly differ from outdoor conditions. Solely by virtue of room occupancy and operation of main openings to enable better solar exposure, users are able to maintain higher temperatures indoors. In addition, the attenuation of thermal oscillation is notorious in this season, and thermal lag is negligible. The relative indoor humidity varies from 50% to 72% and its average value is about 65% (Figure 13), which falls within comfortable ranges (Figure 13).

Simulations were carried out in order to establish illuminance levels and distribution of radiant temperatures using DianaX<sup>®</sup> software.<sup>22</sup> Considering a glass

transmission factor (0.8) and reflection coefficients in the room for the floor (0.4), walls and ceilings (0.6), maximum illumination levels of 5374 lux were found near the glazed balcony and the average value is 2456 lux, thereby achieving satisfactory values for 12 h (Figure 14). In the glazed gallery that surrounds the courtyard, the maximum level is 2695 lux and the average value is 2277 lux. The correlation between mean and maximum values of the gallery (1.20) and the room (2.18) shows that daylight distribution is more uniform in the gallery than in the room, resulting in a more stable, luminous atmosphere.

Theoretical values were also established for radiant temperature simulations: emissivity (0.8) and absorptivity (0.2). Due to the sustainable design features present in this building, the maximum radiant temperature in the glazed balcony and the gallery (Figure 15) is above 17.5°C and 16°C, respectively. The average values are approximately 15.5°C in the room and 16°C in the gallery, which has a more uniform distribution.

### Summer results

During the summer period, it must be taken into consideration that the interior spaces are naturally ventilated during a large part of the day and solar protections are used in order to prevent excessive solar gains. Indoor temperature has a daily variation of 4°C, i.e. from 24°C to 28°C, whilst outdoor temperature has more extreme minimum and maximum levels (Figure 16).

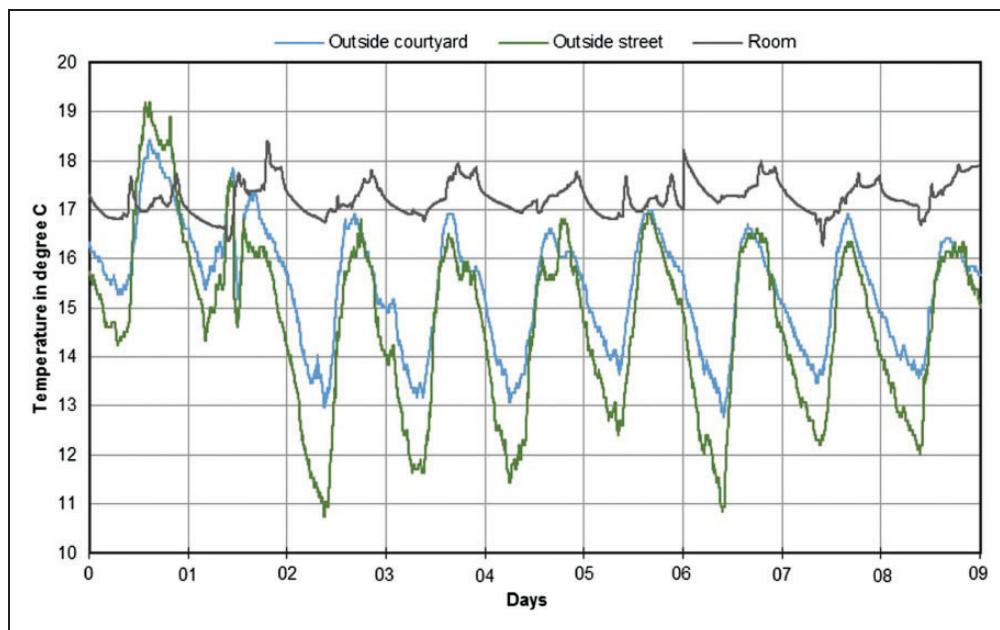


**Figure 12.** Air temperatures in winter.

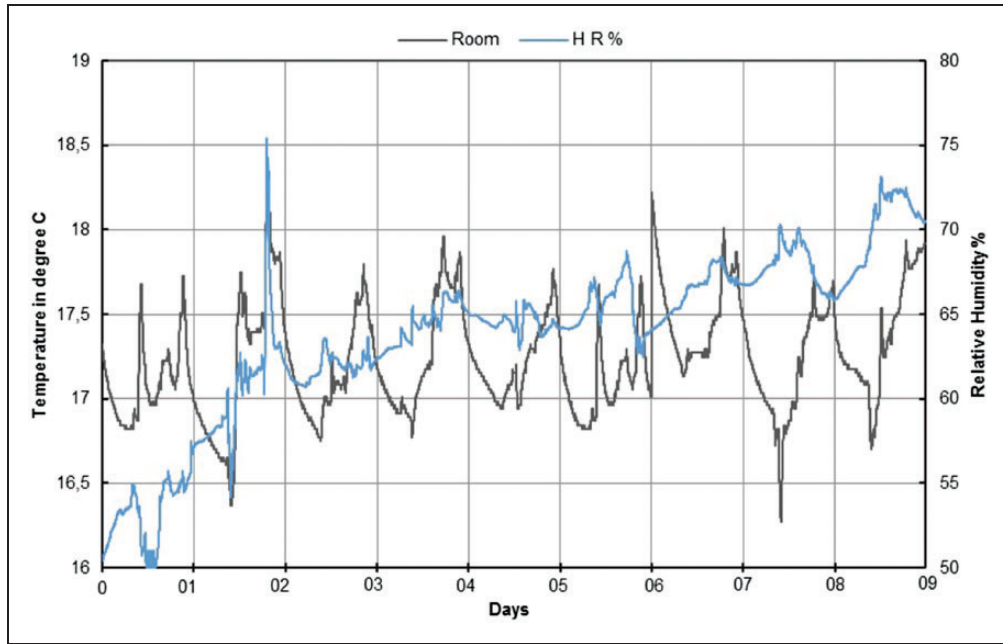


Figure 13. Relative humidity versus air temperature in winter.

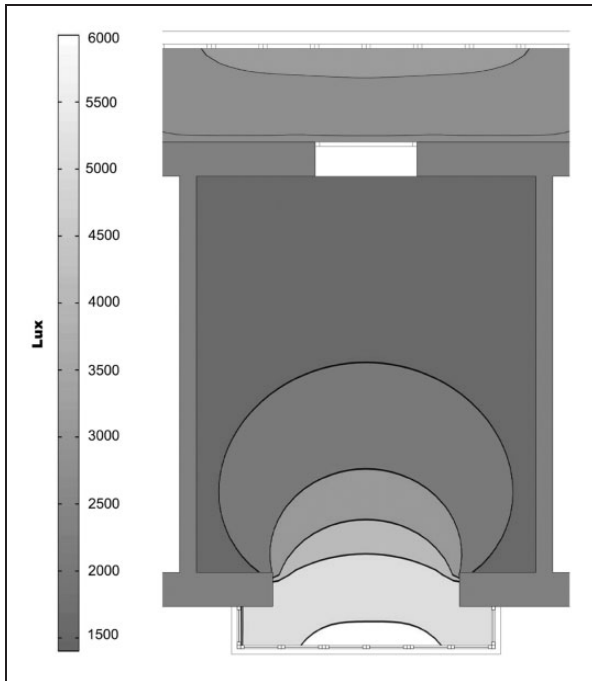


Figure 14. Illumination levels in winter. 12 solar hours.

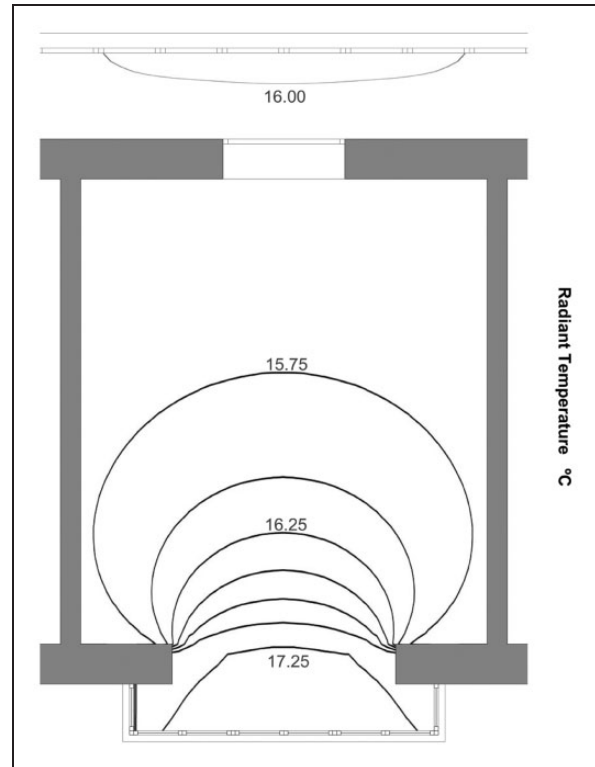
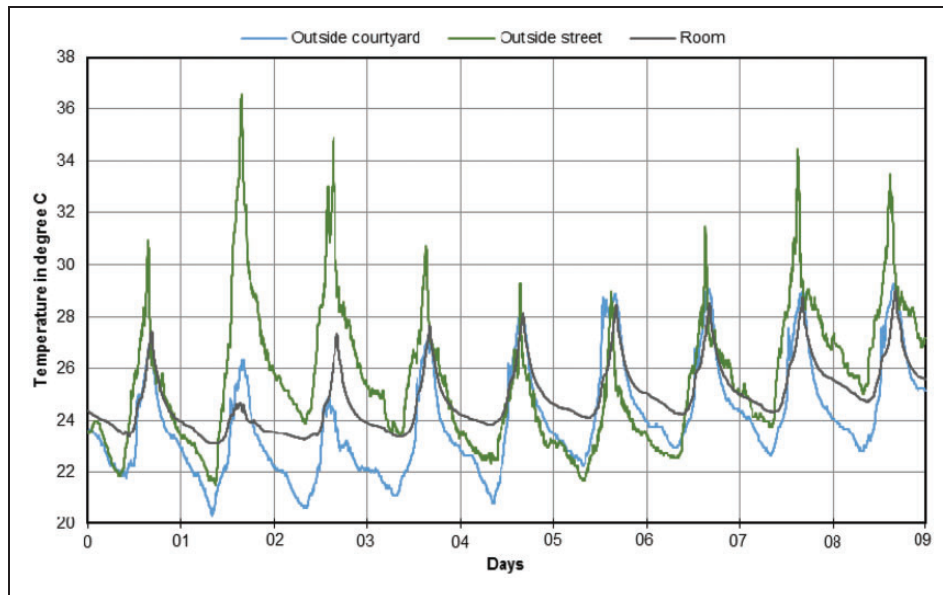
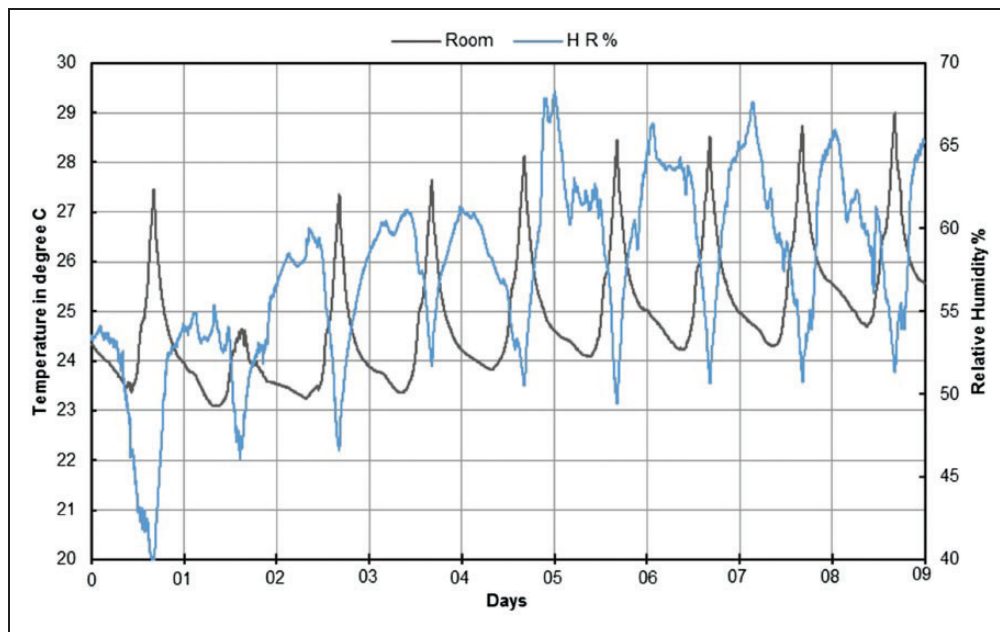


Figure 15. Radiant temperature in winter. 12 solar hours.



**Figure 16.** Air temperature in summer.



**Figure 17.** Relative humidity versus air temperature in summer.

Once again, the interaction between user and environment through architecture modifies indoor conditions by using traditional strategies to achieve comfort. Thermal inertia is influenced by similar indoor and outdoor conditions; although, during the night, walls do

effectively transmit some of their heat gains indoors. The relative indoor humidity varies from 40% to 67%, is inversely proportional to air temperature and has an average value of about 58%, which again is an acceptable value for thermal comfort (Figure 17).

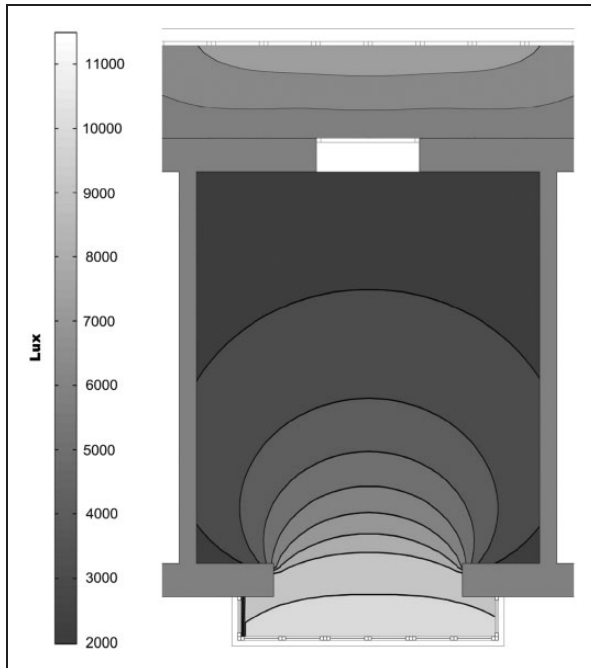


**Figure 18.** Illumination levels in summer. 12 solar hours.

The simulated illumination levels (Figure 18) show a maximum of 11,230 lux near the glazed balcony and 7586 lux in the gallery. The average values are 4331 lux in the room and 6411 lux in the gallery, respectively, and peak values are achieved at 12 h solar time (Figure 19). The use of solar protections plays a key role during this season in preventing sunrays from penetrating the openings. It is a common strategy to use the courtyard as the main source of daylight because higher and more uniform values of illumination (1.20) can be found here, rather than in the street. The maximum radiant temperature in the glazed balcony and the gallery is above 28°C and 26.5°C, respectively. The average values are approximately 25.5°C in the room and 26°C in the gallery (Figure 19). Therefore, there is a risk of overheating, which is not a serious issue as it can easily be counteracted through the use of solar protections and natural ventilation.

### Adaptive comfort model

The adaptive comfort model defined by ASHRAE Standard 55-2013<sup>26</sup> can be used in naturally ventilated spaces where individuals can freely operate windows. The standard assumes that inhabitants will adapt their clothing to thermal conditions (1.0 and 0.5 clo, standard clothing for winter and summer, respectively), and that they are engaged in sedentary activities such as

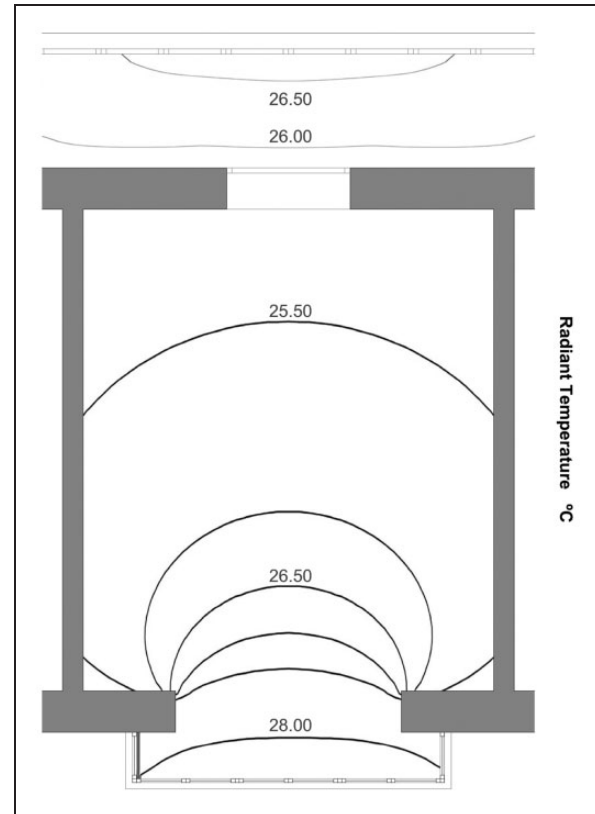


**Figure 19.** Radiant temperature in summer. 12 solar hours.

reading (1.0–1.3 met). Additionally, several studies have established that people who live in naturally ventilated buildings are likely to be more tolerant of variations in thermal conditions.<sup>27,28</sup>

Taking into account records from data loggers in winter, and in spite of the fact that the interior temperatures remain below comfort limits, they can be considered to be close to them (Figure 20). Due to the stability of indoor temperatures, the use of adequate clothing (up to 1.0 clo) and the greater tolerance of people to such conditions, these values can be considered as tolerable and near comfort limits. The urban fabric of Cadiz has greatly adapted to the availability of solar radiation and the prevalent winds and has led to a limit in dimensions of urban canyons that would not be acceptable in a harsher climate. Levels of thermal comfort inside this historic property are very near ideal conditions (Figure 20). In winter, temperatures are just under the lower comfort limit but can still be considered acceptable (around 16–18°C). In summer, comfort is achieved for the majority of hours. These levels have been achieved solely by traditional design techniques.

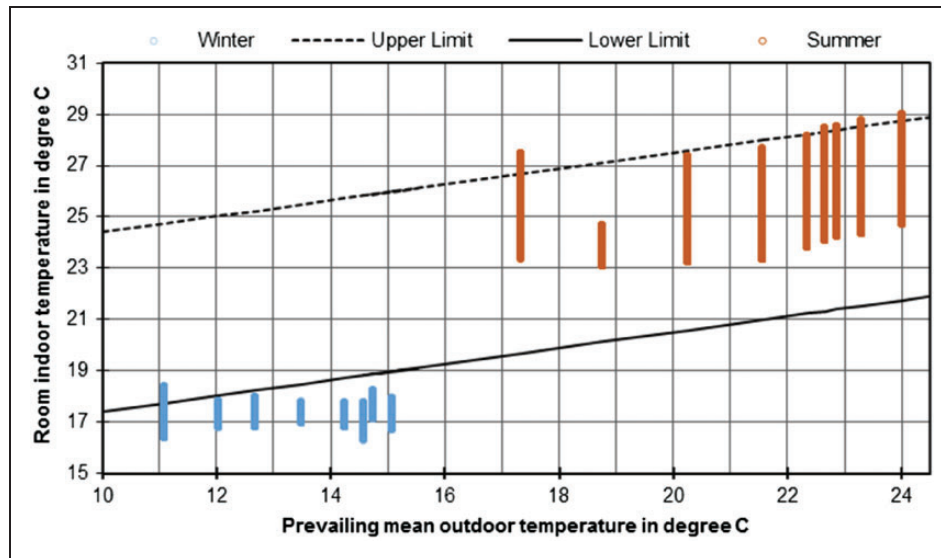


**Figure 20.** Air temperature in an adaptive comfort model during winter and summer.

## Conclusions

The proposed simulation methodology has been proven to be valid under high solar radiation conditions and in dense urban grids with highly reflective materials. Conditions for the open field are not applicable in this case, as the pattern for solar radiation on the façades of these buildings differs greatly. Despite the fact that these dwellings are located in a dense urban grid, this does not represent a burden to solar access; considerable amounts of solar radiation impinge on the façades at different heights, which has a decisive importance on passive strategies for human comfort, such as solar gains and thermal lag.

Simulations and on-site measurements have proven that under mild climates with slight thermal oscillations, a constructive technique that enhances thermal lags, rather than thermal insulation, is highly effective. Complex openings with multiple layers help to amend thermal discomfort by means of solar gains and adaptive ventilation when the envelope does not provide sufficient protection. Levels of RH stay within comfort levels during the vast majority of the year. Porous construction materials and façade openings permit the dissipation of excess humidity. Regarding comfort levels, it can be assured that this historic property could achieve acceptable levels of comfort during the cold and hot seasons. This is not a minor feat given the circumstances. First, this house is located within a very dense urban fabric, and also has a very high FAR, around 400%. In such conditions, it would be expected that poor solar access in winter would make temperatures fall abruptly inside the house; furthermore, in

summer, a dense urban grid can result in a rise in temperatures due to heat island effect. However, in this case, a clever combination of the mild climate and architectural design has contributed to these comfortable conditions.

In this research, on-site measurements have defined the transient thermal behaviour of inhabited dwellings, in which users are able to adapt indoor conditions to achieve an adequate range of comfort. As has been proven, operating openings for improvement of solar exposure in winter or using solar protection and natural ventilation in summer could greatly influence indoor conditions. In winter, the effect of urban and architectural design can be summarized as a reduction in humidity and stabilization in temperature pattern due to solar gains in the courtyard. In summer, peak temperature values are attenuated and levels of RH could vary slightly. Obviously, some degree of discomfort should be expected, but globally speaking, acceptable levels of comfort are achievable solely by means of architectural design and active systems are unnecessary during most of the year (Figure 20).

Our results show that in this case, traditional urban grid and buildings can be creatively adapted to their environmental conditions. The mild climate has perfected this environmental responsiveness throughout history. Such knowledge would contribute to enhancing the urban retrofitting strategies centred on human comfort and environmentally conscious architectural design. Nevertheless, further research is needed to implement these traditional strategies in a modern context. Based on this study, the most important design feature should be preserved and not by only tectonic means, but by environmental consideration. These

conclusions open the path for future research on other similar conglomerates. Although this study is strictly correlated to the intrinsic characteristics of Cadiz, the methodology highlights a number of conclusions useful for other historic cities in the Mediterranean.

In accordance with our findings presented in this article, historic dwellings in the city of Cadiz could in fact achieve conditions close to comfort exclusively by applying traditional design strategies that do not require any artificial or expensive mechanical systems. This is a notable achievement and as per conclusions of this research, it is advisable that these facts be taken into account in all future intervention or modification projects related to these historical properties.

### Authors' contribution

All authors contributed equally in the preparation of this manuscript.

### Acknowledgements

The authors would like to show sincere gratitude to the General Urban Development Plan Office of Cadiz for its support of the fieldwork. The authors also extend sincere gratitude to the Project 150203/EF 'Grupo de investigación en formación. Grupo de Arquitectura y Construcción Sustentable' of the Universidad del Bío-Bío for supporting this research.

### Declaration of conflicting interests

The author(s) declared no potential conflicts of interest with respect to the research, authorship, and/or publication of this article.

### Funding

The author(s) received no financial support for the research, authorship, and/or publication of this article.

### References

- European Commission. *EU energy in figures 2013, statistical pocketbook*. Luxembourg: Publications Office of the European Union, 2013.
- Government of Spain. *Plan energy saving and efficiency action 2011–2020*. Madrid: Spanish Institute for Energy Diversification and Saving, 2011.
- Olgay V. *Design with the climate*. Princeton, NJ: Princeton University Press, 1963.
- Givoni B. *Man, climate and architecture*. Amsterdam/London/New York, NY: Elsevier Publishing Company Limited, 1969.
- Borong L, Gang T, Peng W, Ling S, Yingxin Z and Guangkui Z. Study on the thermal performance of the Chinese traditional vernacular dwellings in Summer. *Energy Build* 2004; 36: 73–79.
- Singh MK, Mahapatra S and Atreya SK. Thermal performance study and evaluation of comfort temperatures in vernacular buildings of north-east India. *Build Environ* 2010; 45: 320–329.
- Dili AS, Naseer MA and Varghese TZ. Passive environment control system of Kerala vernacular residential architecture for a comfortable indoor environment: a qualitative and quantitative analyses. *Energy Build* 2010; 42: 917–927.
- Zhai ZJ and Previtali JM. Ancient vernacular architecture: characteristics categorization and energy performance evaluation. *Energy Build* 2010; 42: 357–365.
- Alonso Monterde M, Gomez Lozano V, Guillen Guillamon I, Higon Calvet J and Lopez-Jimenez PA. Sustainable building strategies on regional scale: proposal for the Valencian region in Spain. *Indoor Built Environ* 2016; 25: 1054–1064.
- Fai S and Sydor M. Building information modelling and the documentation of architectural heritage: between the “typical” and the “specific.” In: *Proc Digit 2013 – Fed 19th Int'l VSMM, 10th Eurographics GCH, 2nd UNESCO Mem World Conf Plus Spec Sess from CAA*, Arqueol 20 al., 2013, vol. 1, pp.731–734.
- Supic P. Vernacular architecture: a lesson of the past for the future. *Energy Build* 1982; 5: 43–54.
- Cañas I and Martín S. Recovery of Spanish vernacular construction as a model of bioclimatic architecture. *Build Environ* 2004; 39: 1477–1495.
- Cabeza-Lainez JM. Lighting features in Japanese traditional architecture. In: Weber W and Yannas S (eds) *Lessons from vernacular architecture*. London: Routledge, 2013, pp.143–154.
- Rubio-Bellido C, Sanchez-Montañes B, Pulido-Arcas JA and Cabeza-Lainez JM. Techniques of environmental analysis applied to the Urban heritage of Cadiz. In: *Third international conference on heritage and sustainable environment*, Oporto, Portugal, 19–22 June 2012, Oporto: Green Lines Institute, pp.629–637.
- Sánchez de la Flor FJ, Álvarez Domínguez S, Molina Félix JL and González Falcón R. Climatic zoning and its application to Spanish building energy performance regulations. *Energy Build* 2008; 40: 1984–1990.
- AEMET, Agencia Estatal de Meteorología, Ministerio de Agricultura, Alimentación y Medio Ambiente, Gobierno de España, <http://www.aemet.es/> (accessed date 11 November 2014).
- Cabeza-Lainez JM and Pulido-Arcas JA. New configuration factors for curved surfaces. *J Quant Spectrosc Radiat Transfer* 2013; 117: 71–80.
- Cabeza-Lainez JM, Pulido-Arcas JA and Castilla MV. New configuration factor between a circle, a sphere and a differential area at random positions. *J Quant Spectrosc Radiat Transfer* 2013; 129: 272–276.
- Cabeza-Lainez JM, Pulido-Arcas JA, Sanchez-Montañes B and Rubio-Bellido C. New configuration factor between a circle and a point-plane at random positions. *Int J Heat Mass Transfer* 2014; 69: 147–150.
- Rubio-Bellido C, Pulido-Arcas JA and Sánchez-Montañes B. A simplified simulation model for predicting radiative transfer in long street canyons under high solar radiation conditions. *Energies* 2015; 8: 13540–13558.
- Jimenez-Verdejo JR, Pulido-Arcas JA and Shuji F. Considerations on formation and transformation of house types in the old quarter of Cadiz. *J Architect Plan* 2015; 80: 2855–2860.
- Cabeza-Lainez JM. *Fundamentos de Transferencia Radiante Luminosa* (including software for simulation). La Coruña: Netbiblo, 2010.
- Cabeza-Lainez JM. Solar radiation in buildings, transfer and simulation procedures. In: Babatunde E (ed.) *Solar radiation*. Rijeka, Croatia: In Tech, 2012, Chapter 16, pp.291–314.
- Catálogo de patrimonio arquitectónico, Plan General de Ordenación Urbana de Cadiz, <http://institucional.cadiz.es/area/Urbanismo/57> (2012, accessed 11 November 2014).
- Gagliano A, Patania F, Nocera F and Signorello C. Assessment of the dynamic thermal performance of massive buildings. *Energy Build* 2014; 72: 361–370.



26. ASHRAE 55-2013. *Thermal environmental conditions for human occupancy*. Atlanta: American Society of Heating, Refrigerating and Air-conditioning Engineers Inc., 2013.
27. Feriadi H and Wong NH. Thermal comfort for naturally ventilated houses in Indonesia. *Energy Build* 2004; 36: 614–626.
28. Bouden C and Ghrab N. An adaptive thermal comfort model for the Tunisian context: a field study results. *Energy Build* 2005; 37: 952–963.
29. Lambert JH. In: DiLaura D (ed.) *Photometria. sive de mensura et gradibus Luminis, Colorum et Umbrae*. IESNA. 2001. 1764.
30. Moon PH (1962) *The Scientific Basis of Illuminating Engineering*. New York: Dover Publications.
31. Yamauchi J (1927) *The Light Flux Distribution of a System of Inter-reflecting Surfaces*. Researches of the Electro-technical Laboratory. No. 190. Tokyo.